

# **Egyptian Journal of Agronomy**

http://agro.journals.ekb.eg/



Evaluating the impact of supplementary irrigation on the WRSI index of rainfed wheat under climate change scenarios in Tabriz, Iran using FLF-LSTM and LARS-WG models



Mouneskhah, Vahid; Samadianfard, Saeed\* and Majnooni-heris, Abolfazl

Water Engineering Department, Faculty of Agriculture, University of Tabriz, Tabriz, Iran

LIMATE change and reduced seasonal rainfall are among the most important factors intensifying water stress in rainfed agricultural systems. The aim of this study is to investigate the effect of climate change on the Water Requirement Satisfaction Index (WRSI) for rainfed wheat in Tabriz during the future time period up to 2100. The LARS-WG statistical model was used to generate future climate data, which was calibrated and run with CNRM-CM6-1 and MPI-ESM1-2-LR, under three SSP126, SSP245, and SSP585 scenarios. These models were selected due to their high ability to reconstruct the region's climate data and are able to simulate changes in temperature and precipitation. Subsequently, the Long short-term memory (LSTM) and Forex Loss Function-LSTM (FLF-LSTM), as deep learning models, were used to predict reference evapotranspiration (ET<sub>0</sub>) values. The LSTM model, as a recurrent neural network-based model, has the ability to identify complex patterns in climate time series. Moreover, the FLF-LSTM model, using a composite loss function, provided more accurate performance compared to the classic LSTM. The error metrics reveal that the FLF-LSTM model outperformed the standalone LSTM in terms of accuracy and reliability, with a root mean square error of 0.71 and a mean bias error of 0.06 during the test period. Additionally, examination of the WRSI in the future time periods and considering climate change scenarios showed that WRSI will have a downward trend under the influence of increased temperature and decreased precipitation. This means an increase in water stress in different growth stages of rainfed wheat. However, the use of supplementary irrigation in sensitive growth stages, especially during the grain filling stage, was able to improve the WRSI and reduce the negative impact of climate change.

 $\textbf{Keywords:} \ Climate \ change, \ Deep \ learning \ models, \ Rainfed \ wheat, \ Supplementary \ irrigation, \ WRSI.$ 

### Introduction

Ensuring the water supply needed for the agricultural sector as the largest consumer of water resources is one of the main concerns of the authorities. The increasing demand for agricultural products due to the increasing population trend and the reduction of available water resources have led to environmental crises. Therefore, examining the optimization of water consumption in the agricultural sector will be of importance. Given the severe limitation of water resources available to the agricultural sector, providing solutions to increase water use efficiency will be crucial. One of the solutions to address the problem of meeting the water needs in the agricultural sector is deficit irrigation of irrigated lands or increasing the production of rain-fed crops through supplementary irrigation. Deficit irrigation is a strategy in which less water than the potential evapotranspiration and maximum yield is used, resulting in the conservation of limited water resources (English and Raja, 1996) and an increase in water use efficiency (Fereres and Soriano, 2007). The purpose of supplementary irrigation is also the application of a limited amount of water during the end of rainfall to maintain plant growth. However, this amount of water alone is not sufficient for adequate production (Tavakoli and Oweis, 2004), and its amount is also determined based on the climatic conditions of the cropping season (Oweis and Hachum, 2009). However, in selecting the appropriate time for supplementary irrigation, attention to the critical growth stages of the crop in relation to water stress is important. In fact, supplementary irrigation refers to the consumption of a limited amount of water in the crop plant during the time of rainfall shortage to provide sufficient water for plant growth in order to increase and stabilize the yield. Therefore, the essential feature of the supplementary irrigation is the complementary nature of rainfall along with the application of irrigation. In areas where the amount

 $*Corresponding \ author \ email: s.samadian@tabrizu.ac.ir$ 

Received: 13/05/2025: Accepted: 01/10/2025 DOI: 10.21608/AGRO.2025.384725.1695

©2025 National Information and Documentation Center (NIDOC)

and temporal distribution of rainfall is unfavorable, supplementary irrigation is recommended for optimal production of rain-fed crops (Oweis 1997). In recent years, research findings have shown that implementing supplementary irrigation increased the yield of rain-fed cereals (Erekul et al., 2012). One of the limitations in the implementation of supplementary irrigation is providing the required water. In addition, the limitation of water resources has resulted in the available water in the agricultural sector being less than the water needs of the cultivated crops. Therefore, attention to the optimal distribution of limited water throughout the growing season, considering the sensitivity of crops to stress at different growth stages, can be considered as an appropriate tool to increase water use efficiency. Tarnawski and et al. (2018) studied the sensitivity of the modified water satisfaction index model to the amount of rainfall. agrometeorological hazards of corn production in the Tanzania region. They used water WRSI simulation to identify water-stressed areas in the Tanzanian corn cultivation region with other fixed factors (diversity, fertilizer use, pests, diseases, etc.) and reported the relationship between the WRSI, seasonal rainfall and average soil moisture with national corn yield.

Climate change and its impacts on rainfed agriculture and water resources have become an important research topic in recent decades (Sadek & Saba, 2011; Abo-Yousef, et al., 2024). Numerous studies around the world have shown that rising temperatures and declining rainfall directly affect the yield of rainfed crops and plant water requirements. One of the most important indicators for assessing the level of plant water requirements under different climatic conditions is the Water Satisfaction Index (WRSI). WRSI is widely used in assessing water stress and predicting plant water requirements under climate change conditions. Doorenbos and Kassam (1979) first introduced the WRSI and used it to predict the performance of agricultural crops under drought and water scarcity conditions. This index has found widespread application, especially in dry and semi-dry regions where rainfed agriculture is prevalent. Additionally, Lobell et al. (2011) conducted research on the impact of climate change on rainfed agriculture and their results showed that climate changes in South Asia and North Africa have led to a decrease in the yield of rainfed crops, especially under water scarcity and drought conditions. Furthermore, Schlenker and Roberts (2009) showed that the performance of rainfed crops in severe drought conditions decreases using climate change models and this decrease in performance is more evident especially in tropical and arid regions. Chen et al. z(2025)shown that CNRM-CM6-1, has HadGEM3-GC31-LL, MPI-ESM1-2-LR and MRI-ESM2-0 from the CMIP6 project have been

effective in simulating plant water needs and assessing the impacts of climate change in different agricultural regions. These models are capable of simulating temperature and precipitation changes in different agricultural regions and can help more accurate prediction of plant water needs and water resource management. So, the aim of this study is the assessment of the effect of climate change on rainfed wheat Water Requirement Satisfaction Index under representative concentration pathways scenarios (RCP 4.5 and RCP 8.5) to tackle future agricultural challenges. For such a purpose, we present an innovative Forex Loss Function-Long Short-Term Memory (FLF-LSTM) model, a deep learning model with the aim of improving the accuracy of evapotranspiration and allowing one to determine particular supplementary irrigation needs. The innovation of this research is to combine new machine learning approaches with new climate scenarios to acquire more sophisticated water management policies and allow climate adaptation in the future.

The precipitation and temperature were deliberately chosen as the driving inputs of the above-described LSTM and FLF-LSTM networks. They are the most important climatic drivers of water taken up by crops and are annually provided through past observation and future climatic scenario outcomes, respectively. Using them allows simplifications of model structures, program clarity, and reduction of uncertainty in the input, almost entirely under longterm scenarios where sufficient data of the microclimatic variables like wind speed, relative humidity, and solar radiation are not always With choosing precipitation and available. temperature, the study maintain a balance among model accuracy and practical applicability under long-term climatic studies.

## Materials and Methods Study area

The study area of the current research is Tabriz plain, located in East Azerbaijan Province in the northwest of Iran (Figure 1). This region is located at a geographic position of about 38 degrees north latitude and 46.3 degrees east longitude and has a cold semi-arid climate. The annual rainfall in this region is about 250 millimeters and the annual average temperature is about 12 degrees Celsius (Khosravi et al., 2020). Agriculture in this region is mainly carried out as rain-fed. Due to the high dependence of rain-fed agriculture on precipitation, the evaluation of the impact of climate change on water supply indicators such as WRSI in this region is of high importance. Therfore, daily climatic data including precipitation, minimum and maximum temperature, solar radiation, relative humidity, and wind speed for the baseline time period of 1990-2020 were collected from the Tabriz meteorological station.

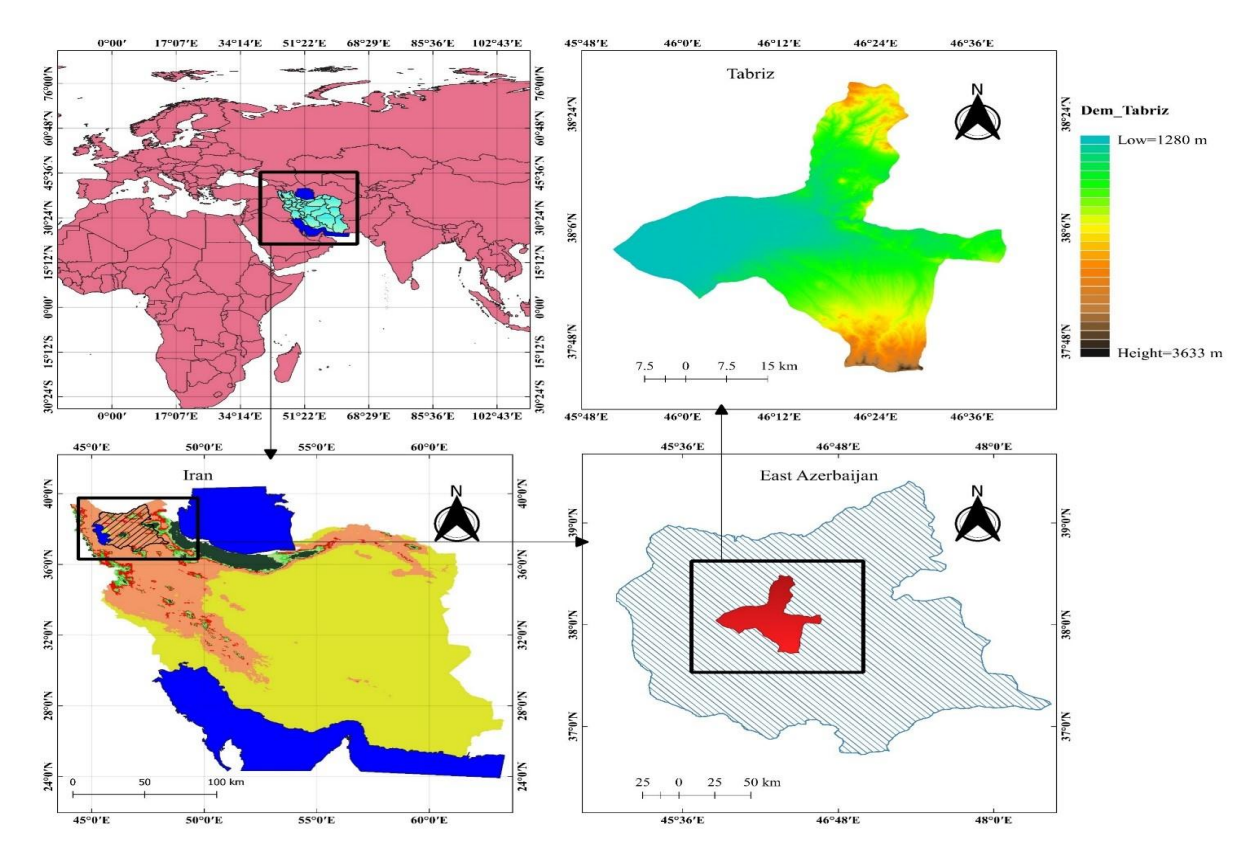


Fig. 1. The location of the study area (Talebi and Samadianfard, 2024).

#### The LARS-WG model

The LARS-WG model is a statistical model based on the simulation of daily climate data, which can produce data with similar statistical characteristics in the future time periods using the statistical distributions of observed climate data. The model should be calibrated with baseline data and then it may be used for the future period to simulate climate data (Semenov & Stratonovitch, 2010). Once calibrated, the model generates synthetic weather data that mirrors the historical record's statistical features, such as means, variances, and frequencies of extreme events. This methodology enables researchers to analyze potential climate impacts on a local scale, providing a more detailed understanding of how climate change could manifest in specific regions. The outputs produced LARS-WG are invaluable for diverse applications, including agricultural planning, water resource management, and ecological studies. By simulating daily precipitation, temperature, and solar radiation, the model aids in assessing agricultural yields under future climate scenarios, guiding adaptive strategies in crop management to ensure food security. Moreover, its capability to replicate daily weather sequences makes it useful for hydrological modeling, predicting future water availability challenges. Furthermore, LARS-WG's role in downscaling broad-scale climate models into

localized predictions enhances its utility in environmental assessments.

The MPI-ESM1-2-LR and CNRM-CM6-1 are two prominent climate models that play critical roles in forecasting future climate scenarios under varying greenhouse gas emissions pathways (Giorgetta et al., 2013). The MPI-ESM1-2-LR, developed by the Max Planck Institute for Meteorology, is part of the Earth System Model series that incorporates interactions across the atmosphere, ocean, land surface, and biosphere. This model boasts advanced atmospheric dynamics and coupling techniques, enabling it to simulate climate processes with high precision, making it integral for studies that assess long-term climate stability and variability. Conversely, the CNRM-CM6-1, developed by the Centre National de Recherches Météorologiques, is part of the sixth phase of the Climate Model Intercomparison Project (CMIP6). It features refined parameterizations for cloud processes and improved resolution in atmospheric components, allowing for more accurate predictions of rainfall patterns occurrences and extreme weather (Voldoire et al., 2019). Both models are crucial for examining the impacts of climate change on global and regional scales, providing nuanced insights into temperature and precipitation trends (Kouadio, L., et al., 2023).

# Estimation of reference evapotranspiration with LSTM and FLF-LSTM models

In this research, two deep learning models based on recurrent neural networks were used to accurately estimate the reference evapotranspiration (ET $_0$ ) in the Tabriz region: the LSTM model and the FLF-LSTM model. These two models were used to predict ET $_0$  using multi-year climate data and to increase the accuracy of the WRSI prediction. Instead of using the Penman-Monteith formula, these two models were used to estimate the ET $_0$  more accurately (Zhang et al., 2023; Chen et al., 2023).

#### LSTM and FLF-LSTM models

LSTM is a type of recurrent neural network (RNN) that has the ability to store and recall information over long time periods. This feature has made LSTM a powerful tool for analyzing time series such as temperature, humidity, wind speed, radiation, and other climatic parameters. The internal structure of LSTM consists of a memory cell, an input gate, an output gate, and a forget gate, which allow the model to model complex temporal dependencies well. In this study, daily climatic data including maximum and minimum temperature, solar radiation were used as inputs and the daily ET<sub>0</sub> value was considered as the model output. The models were trained based on historical data. Then, using simulated climate data, ET<sub>0</sub> for future periods was predicted. The LSTM model was implemented in the Python environment. The data were divided 70% for training and 30% for testing, and error criteria were used to evaluate the prediction accuracy. Additionally, the Forex Loss Function-LSTM (FLF-LSTM) is an advanced version of the LSTM neural network that is designed to improve the accuracy in predicting continuous time series. The main feature of this model is the use of the custom Forex Loss function. This loss function assigns different weights to underestimation and overestimation errors, instead of uniform error evaluation.

In climate applications such as ET<sub>0</sub> forecasting, underestimation errors can have greater negative impacts on agricultural decision-making. The Forex Loss Function accounts for this asymmetry and, by adjusting a weighting parameter (a), allows the model to be more sensitive to a particular type of error during training. The implementation of this model was utilized by Python environment and deep learning libraries like TensorFlow and Keras. Climate data, including temperature, solar radiation, relative humidity, and wind speed, were defined as model inputs. The model trained with the Forex Loss Function demonstrated better performance in accurately reconstructing evapotranspiration patterns and reducing forecast error compared to the standard LSTM model (Zhang et al. 2022). The  $\alpha$  parameter is the weighting factor for the underestimation error, which is determined using the Grid Search method. To tune the  $\alpha$  parameter in the Forex Loss function, the Grid Search method with cross-validation was employed. Different  $\alpha$  values in the range of 0.3 to 0.7 were tested, and the model was trained for each value. After statistical analysis of the results, the value of  $\alpha$ =0.6 was selected as the optimal value with the lowest RMSE and MAE.

# Crop coefficient $(K_c)$ and root development depth

In this study, the Growing Degree Day (GDD) was used to determine the plant's phenological stages and calculate the crop coefficient ( $K_c$ ). The GDD index specifies the cumulative heat required for the plant's growth and development from the germination stage to full maturity. GDD was calculated using the following equation

$$GDD = \frac{(T_{max} + T_{min})}{2} - T_{base}$$
 (1)

where,  $T_{max}$  is daily maximum temperature (°C),  $T_{min}$  is daily minimum temperature (°C) and  $T_{base}$ denotes base or threshold temperature below which plant growth is negligible or zero. The  $T_{base}$  is one of the key parameters in calculating the GDD index. This parameter represents the temperature threshold below which plant growth is stopped or occurs very slowly. Accurate selection of the Tbase value for each crop is of high importance, as it directly affects the accuracy of growth modeling and phenological requirements. Regarding wheat, McMaster and Wilhelm (1997) considered the base temperature for winter wheat equivalent to zero degrees Celsius. This value has also been empirically confirmed by Bauer et al. (1984) in the Great Plains region of the United States. So, in this study, the T<sub>base</sub> was also considered to be zero. The GDD for wheat may vary depending on the climatic and geographical conditions of the region. In some areas, like Tabriz with a semi-arid climate temperature and precipitation specific conditions, the GDD for wheat may be higher than the usual values mentioned for other regions. In regions with with hotter summers and a longer growing season, the plant will require higher temperatures to reach the maturity stage. Therefore, in these areas, a higher GDD value for wheat can be reported. According to climate reports, in the Tabriz, the GDD for wheat during the growth period may reach 2,200 or even more, especially if the growing season is longer and the temperature conditions are more favorable for the plant. This higher value indicates a longer growing season in Tabriz, where wheat requires higher temperatures to reach the maturity stage. For each stage, the appropriate K<sub>c</sub> was extracted from reliable sources (such as FAO56) and used in the calculation of the crop evapotranspiration (ET<sub>c</sub>). Furthermore, with the increase in GDD throughout the season, the root depth development was also increased. The root depth development started at 0.4 meters at the beginning of growth and gradually expanded to approximately 1.04 meters at the final maturity stage, which was effective in calculating the available soil moisture storage.

This GDD-based approach allowed for a more precise timing of K<sub>c</sub> allocation and root depth in the WRSI model, especially under climate change conditions where the growing season length and air temperature undergo significant changes. Moreover, the K<sub>c</sub> was determined in a stage-wise manner using the GDD. The phenological growth stages of the plant (germination, vegetative growth, flowering, and maturity) were differentiated using GDD thresholds, and appropriate K<sub>c</sub> values were assigned for each stage (Allen et al., 1998). Additionally, the root depth development was calculated linearly using the GDD values, which plays a key role in determining the available water storage capacity for the plant.

For the calculation of Total Available Water (TAW) in wheat, the root depth is one of the critical parameters. A root depth of 1 meter was considered for wheat, but this value may vary depending on the environmental conditions and irrigation. A linear model was used to calculate the daily root growth.

## Water Requirement Satisfaction Index (WRSI)

The Food and Agriculture Organization of the United Nations (FAO) has developed the Water Requirement Satisfaction Index (WRSI) as a usable model to estimate agricultural production using rainfall in areas of the world facing water scarcity (Frere and Popov, 1986). In rainfed agriculture, the source of the required soil moisture is rainfall plus available soil water. If rainfall exceeds the plant's water requirement, it is used to replenish the available soil moisture, and if it exceeds the capacity to refill the soil water content, it is lost as runoff and deep percolation. However, if the plant's water requirement exceeds the rainfall, the available soil water will be used to compensate for the rainfall deficit, and if insufficient, a moisture deficit will be recorded. In this study, the basis for the moisture balance calculations was considered as 10-day time steps. At the end of the growing season, the WRSI is expressed as a percentage of the total water requirement satisfied by rainfall and available soil moisture. Therefore, WRSI is an indicator of water availability performance for the crop in 10-day time steps during the growing season, which is a function of rainfall, evapotranspiration, soil type, and crop type. The value of this index varies from 0, where the crop's water requirement is never satisfied, to 100%, where the water requirement is fully satisfied

(Sultan et al., 2010). Quantitative values such as 40% or 50% indicate crop failure (Verdin and Klaver, 2002). Silva et al. (2010) classified WRSI into three categories: values above 50% have low climatic risk, between 40-50% have moderate climatic risk, and less than 40% have high climatic risk. The WRSI is used to analyze the extent to which the plant's water requirement is met during the growing season and is calculated from the following formula (Verdin and Klaver, 2002).

$$\Delta W_i = R_i + S_i - ET_{C_i} \tag{2}$$

where  $\Delta W_i$  is the moisture deficit (negative sign) or moisture surplus (positive sign) in the i-th decade in millimeters,  $\mathbf{R}_{i}$  is the rainfall in the i-th decade in millimeters,  $S_i$  is the available moisture at the beginning of the i-th decade in millimeters, and ET<sub>G</sub> is the evapotranspiration of the crop under standard conditions in the i-th decade in millimeters. To the calculate standard evapotranspiration values, the FAO Penman-Monteith method and crop coefficients throughout the growing season were used, and the standard evapotranspiration was calculated using the following equation (Allen et al., 1998):

$$ET_{c_i} = ET_{0_i} \times K_{c_i} \tag{3}$$

where  $ET_{0i}$  and  $ET_{ci}$  are the reference and standard evapotranspiration of the crop in the i-th decade in millimeters, respectively, and  $K_{ci}$  is the crop coefficient. It should be noted that the daily crop coefficients during the growing season were calculated by combining the information from FAO publication 56 and regional data. If there is an agricultural water deficit, the cumulative agricultural water satisfaction will be calculated using equation 4, and otherwise using equation 5.

$$CWS_i = CWS_{i-1} + ET_{C_i} + \Delta W_i$$
 (4)

$$CWS_{i} = CWS_{i-1} + ET_{C_{i}}$$
(5)

The excess water also escapes the plant's reach through runoff and/or deep percolation, and ultimately the soil moisture available was corrected using equation 6:

$$S_{i+1} = S_i + R_i - ET_{C_i} \tag{6}$$

It should be noted that the range of variations in available soil moisture will vary between the minimum value of zero and the maximum value of the soil water holding capacity (considering the root depth). The agricultural water satisfaction index for the desired n-th decade was obtained from equation 7.

equation 7.  

$$WRIS_{n} = \frac{cws_{n}}{\sum_{i=1}^{n} ET_{C_{i}}}$$
(7)

Finally, the average WRSI during the growing season was obtained using equation 8.

$$\overline{\text{WRSI}} = \sum_{i=1}^{n} \frac{\text{cws}_i}{\sum_{i=1}^{n} \text{ETC}_i} \times \frac{1}{n}$$
 (8)

The WRSI values were classified and analyzed into four main categorie. 1) WRSI > 80, full water supply, suitable growth conditions. 2) 60 < WRSI < 80, mild stress, possible minor yield reduction, 3)  $40 < WRSI \le 60$ , moderate stress, significant yield reduction. 4) WRSI  $\leq$  40, severe stress, possible serious crop damage.

#### **Supplementary irrigation**

Supplementary irrigation refers to additional irrigation that is applied when rainfall is not sufficient to meet the water needs of the crop. This type of irrigation can be used at different stages of plant growth (Fouad, 2018). But for rainfed wheat, supplementary irrigation is usually more important at specific stages of growth. In semi-arid climatic conditions like the Tabriz region, rainfed agriculture faces serious challenges due to limited rainfall, poor temporal distribution of precipitation, and consecutive droughts. In such conditions, the use of supplementary irrigation as a management approach plays a key role in maintaining and sustaining production (Pala et al., 2007; Farre & Faci, 2006).

Autumn irrigation, especially at the time of sowing or immediately after, is carried out to provide moisture in the seed establishment zone. This type of irrigation increases the germination percentage, uniform plant establishment, and reduces earlyseason stresses. The study by Soltani et al. (2012) showed that applying one irrigation in the fall led to an increase in the density of germination and ultimately an increase in the final yield of rainfed wheat. Moreover, the report by Zhang et al. (2006) indicates that initial irrigation, especially under uncertain autumn rainfall conditions, can play a key role in compensating for the risk of delayed germination. Moreover, Spring irrigation is typically applied during the critical grain filling stage or early flowering stage. This growth stage is one of the most sensitive periods of the plant to drought stress, which directly affects thousandgrain weight, number of grains per spike, and final vield (Farre & Faci, 2006). Additionally, Pala et al. (2007) reported that applying a single irrigation during the grain filling stage in rainfed wheat increased yield by up to 30%. Furthermore, analytical data based on the WRSI shows that in most growing seasons, this index value falls below 50% in the spring, confirming the need for supplementary irrigation.

#### Evaluation metrics

To evaluate model performance, multiple widely recognized statistical metrics were employed. These include Root Mean Square Error (RMSE), Mean Absolute Error (MAE), Coefficient Determination (R<sup>2</sup>), Mean Bias Error (MBE), Nash-Sutcliffe Efficiency (NSE), and Willmott's Index of Agreement (WI). The statistical quantities are computed as follows:

$$RMSE = \sqrt{\frac{\sum_{i=1}^{n} (p_{i} - o_{i})^{2}}{n}}$$

$$MAE = \frac{\sum_{i=1}^{n} |p_{i} - o_{i}|}{n}$$

$$R^{2} = \left[\frac{\sum_{i=1}^{n} (o_{i} - \overline{o}_{i})(p_{i} - \overline{p}_{i})}{\sum_{i=1}^{n} (o_{i} - \overline{o})^{2} \sum_{i=1}^{n} (p_{i} - \overline{p}_{i})^{2}}\right]^{2}$$
(11)

$$MAE = \frac{\sum_{i=1}^{n} |P_i - O_i|}{n}$$
 (10)

$$R^{2} = \left[ \frac{\sum_{i=1}^{n} (o_{i} - \overline{o}_{i}) (p_{i} - \overline{p}_{i})}{\sum_{i=1}^{n} (o_{i} - \overline{o})^{2} \sum_{i=1}^{n} (p_{i} - \overline{p}_{i})^{2}} \right]^{2}$$
(11)

$$MBE = \frac{1}{n} \sum_{i=1}^{n} (P_i - O_i)$$
 (12)

NSE = 
$$1 - \frac{\sum_{i=1}^{n} (o_i - p_i)^2}{\sum_{i=1}^{n} (o_i - \overline{o}_i)^2}$$
 (13)

WI = 1 - 
$$\left[\frac{\sum_{i=1}^{n}(P_{i}-O_{i})^{2}}{\sum_{i=1}^{n}(|P_{i}-\overline{O}_{i}|+|O_{i}-\overline{O}|)^{2}}\right]$$
 (14)

where  $O_i$  denotes values,  $\overline{O}$ , their observed mean,  $P_i$  the corresponding predicted values, and n the number of observations.

#### Results and discussion

The current research evaluates supplementary irrigation schedules under the SSP2-4.5 scenario utilizing two climate models: CNRM-CM6-1 and MPI-ESM1-2LR. The methodology incorporates advanced computational modeling techniques to simulate the effects of forecasted climate changes on the water requirements of rainfed wheat. WRSI is employed as the primary metric to assess decadal variations in water demand. Initially, GDD are calculated to estimate crop phenology, using temperature data to capture the cumulative heat required for wheat development. The computation of WRSI involves integrating climatic inputs, precipitation including and potential evapotranspiration, to model the water balance over the growing season. The models generate decadal forecasts of WRSI, factoring in climatic variability and its impact on water needs. These forecasts are organized into designated decadal periods (2021-2100), providing a framework for comprehensive comparisons as climatic conditions evolve. To determine the supplementary irrigation required, simulations identify the shortfall in water availability by comparing forecasted WRSI with target values necessary for optimal crop yield. The added supplementary irrigation is calculated by estimating the depth of water needed to bridge this gap. Following the application of supplementary irrigation, the modified WRSI reflects adjustments in water demand satisfaction, confirming the effectiveness of irrigation interventions. Data analysis is facilitated through Python, employing

libraries such as pandas for data manipulation and numpy for numerical computations. An iterative cycle of model testing and refinement ensures that simulations account for climate-induced variability in water demand. To predict the water requirements of rainfed crops under climate change conditions, the LSTM and FLF-LSTM models were used. These models were able to make accurate predictions of evapotranspiration (ET) and crop water requirements in future years. The results showed that the FLF-LSTM model provided higher accuracy in the relevant predictions compared to LSTM. The LSTM model, which is designed for time series predictions, performed well in simulating changes in evapotranspiration and water requirements of rainfed crops. Composite loss functions in time series prediction models, especially in the field of climate, have seen significant growth. In this regard, Wang et al. (2021) improved the performance of LSTM models in predicting complex time series by designing a composite loss function including MSE along with derivative components. They showed that adding components such as gradient-based terms to the loss function can reduce structural error and improve the generalization of the model. In the present study, the Forex Loss Function was used as a custom loss function, which includes not only numerical error but also differences in data

gradients and model oscillation stability. This loss function was able to increase the model accuracy compared to the basic LSTM version, especially in predicting ET<sub>0</sub> under climate change conditions. In Table 1, the comparison between the performance of the base LSTM model and the modified FLF-LSTM in estimating daily ET<sub>0</sub> values over the baseline time period of 1990-2020 showed that the hybrid FLF-LSTM model illustrated better performance. This result is in line with the findings of the study by Wang et al. (2021) and emphasizes that adding structural dimensions to the loss function will be very effective in modeling phenomena that are inherently trending and oscillating, such as evapotranspiration. In another study, Chen et al. (2023) used a composite loss and LSTM models to function evapotranspiration in arid regions of China and showed that adding structural components to the loss function improves the prediction accuracy by more than 15%. The findings of this study also confirm that the performance of the hybrid FLF-LSTM, which has better ability to reconstruct the patterns of daily changes and the temporal continuity of the data. Therefore, it can be concluded that the use of composite FLF not only reduces the numerical error of the model, but also helps to reconstruct a more realistic climate behavior.

Table 1. Error meters of implemented LSTM and FLF-LSTM models.

		FLF-LSTM	Table 1. E	rror meters of
	Test Metrics	Train Metrics	Test Metrics	Train Metrics
RMSE	0.71	0.71	0.72	0.72
MAE	0.54	0.53	0.55	0.55
$\mathbb{R}^2$	0.93	0.93	0.93	0.93
MBE	0.06	0.04	0.02	0.002
NSE	0.93	0.93	0.93	0.93
WI	0.98	0.98	0.98	0.98

In evaluating the impact of climate change on rainfed agriculture in semi-arid regions like Tabriz, the correct selection of the climate model (GCM) and greenhouse gas emission scenario plays a key role in increasing the accuracy of predictions. In this study, two selected models from CMIP6 were examined in three different scenarios of SSP1-2.6, SSP2-4.5, and SSP5-8.5. Also, the CNRM and MIP models, due to their dynamic structure, have been able to better represent regional phenomena in the mountainous areas of Iran and has reconstructed the temperature and rainfall variations of Tabriz with higher consistency. In the examination of emission scenarios, the SSP2-4.5 is recommended as a moderate and more realistic option compared to other scenarios by most global sources and domestic studies. While SSP1-2.6 is highly

optimistic and dependent on severe international actions to reduce greenhouse gases, and SSP5-8.5 depicts the most severe uncontrolled emission path, the SSP2-4.5 offers the most likely path for medium and long-term predictions based on current trends and limited mitigation actions. Therefore, for the continuation of climate analysis in the Tabriz region, including the simulation of sensitive indices such as WRSI, it is recommended to use the CNRM-CM6-1 model along with the SSP2-4.5 scenario as the basis for prediction and risk analysis.

The WRSI is a performance indicator per available water during the growing season and a suitable criterion for evaluating the performance under water scarcity conditions. Figure 2 shows the changes in the WRSI for wheat over an 80-year

statistical period of 2020-2100. According to the results, the average WRSI for wheat in each of the ten studied agricultural years was 65 percent. It should be noted that the calculated values of the WRSI for wheat were calculated solely using rainwater and soil moisture in the root development zone, and any supplementary irrigation pattern would increase the WRSI index.

In the current study, considering the data generated under climate change, decreasing rainfall trends, increasing temperature, increasing ET<sub>0</sub>, and decreasing soil moisture resulted in a decrease in the WRSI value in future periods. These changes were analyzed at the regional level, and water stress trends for rainfed crops were investigated in different time periods. In all scenarios, the increase in temperature and the decrease in precipitation caused a decrease in WRSI for rainfed crops. In the pessimistic scenarios, the WRSI during different growth periods decreased, indicating an increase in water stress and a negative impact on crop yield. These findings suggest that future climate change, especially in semi-arid regions like Tabriz, can pose a serious threat to rainfed agriculture. By comparing the ten-year changes in evapotranspiration, temperature, precipitation, and the WRSI in Figure 2, it can be concluded that the MPI model is less affected by climatic fluctuations compared to CNRM, and the changes in both models are more influenced by precipitation fluctuations, producing a similar trend. Therefore, implementing supplementary irrigation compensate for the lack of precipitation, especially in times of stress, will greatly help improve the WRSI and, consequently, improve yield, as shown in Tables 2 and 3 for both models and three scenarios, before and after irrigation, in the form of a ten-year average.

It can be comprehended from Figure 2 that the WRSI values in the absence of supplementary irrigation show a decrease over time in all climate scenarios including SSP1-2.6, SSP2-4.5, and SSP5-8.5. In the pessimistic scenario SSP5-8.5, the WRSI decrease is more severe and approaches critical values in the final decades (2090-2100). This trend to rising temperatures, decreasing precipitation, increasing ET<sub>0</sub>, and decreasing soil moisture. In the early decades such as 2021-2030, the WRSI value is within the acceptable range (above 60%) in most models, but a decreasing trend is evident in the middle and final decades So, the supplementary irrigation, especially during the grain filling stage, is recommended for rainfed wheat. When WRSI is severely reduced, supplementary irrigation can play a crucial role in maintaining crop yield and reducing water stressrelated damages. The percentage increase in WRSI due to supplementary irrigation was reported to be over 25% in some cases, indicating the plant's

positive response to moisture supply during critical the growth With application stages. WRSI values supplementary irrigation, the increased in all scenarios and models. An increase of 10 to 20% or more was observed in many decades, highlighting the vital role supplementary irrigation in reducing water stress effects. Specifically, in the MPI-ESM1-2-LR model and the SSP5-8.5 scenario, the WRSI value without irrigation was around 0.55, which increased to about 0.69 with irrigation. Figures 3 and 4 show the trend of changes in the WRSI values before and after supplementary irrigation.

In Figure 3, the baseline scenario is observed where the WRSI reflects natural precipitation patterns and inherent variations. Differences across growing seasons reveal how rainfed wheat is impacted by varying levels of precipitation, with some periods that might showing deficits stress development. In contrast, Figure 4 demonstrates the effects of implementing supplementary irrigation, highlighting how these interventions help stabilize the WRSI index. This strategy softens natural rainfall fluctuations and secures adequate moisture levels essential for optimal crop growth. Furthermore, examination of these figures reveals the critical role of supplementary irrigation in leveling the variability seen in Figure 3. The supplementary irrigation appears to buffer against the peaks and troughs of the index, indicating a more consistent and reliable crop water supply. Particularly during drought-prone periods or in the late stages of the growing season, supplementary irrigation seems to prevent drops in water demand satisfaction, suggesting enhanced resilience and potential yield stability. Additionally, Figure 5 presens 10-year changes in WRSI before and after supplementary irrigation for all examined climate change scenarios.

At Figure 5, the WRSI exhibits significant fluctuations when crops rely solely on natural rainfall, indicating periods of potential water stress that can affect plant growth and yield stability. After the implementation of supplementary irrigation, the WRSI trend reflects marked stability. The index values are notably closer to optimal levels, highlighting how irrigation can mitigate the challenges presented by natural rainfall variability. Furthermore, Tables 2 and 3 present the supplementary irrigation schedules based on the WRSI values as calculated by the CNRM-CM6-1 and the MPI-ESM1-2LR models, respectively, under the SSP2-4.5 scenario. These tables detail the values before and after irrigation applications, the supplementary irrigation amounts in millimeters, and specify the autumn irrigation requirements for each decade across the century.

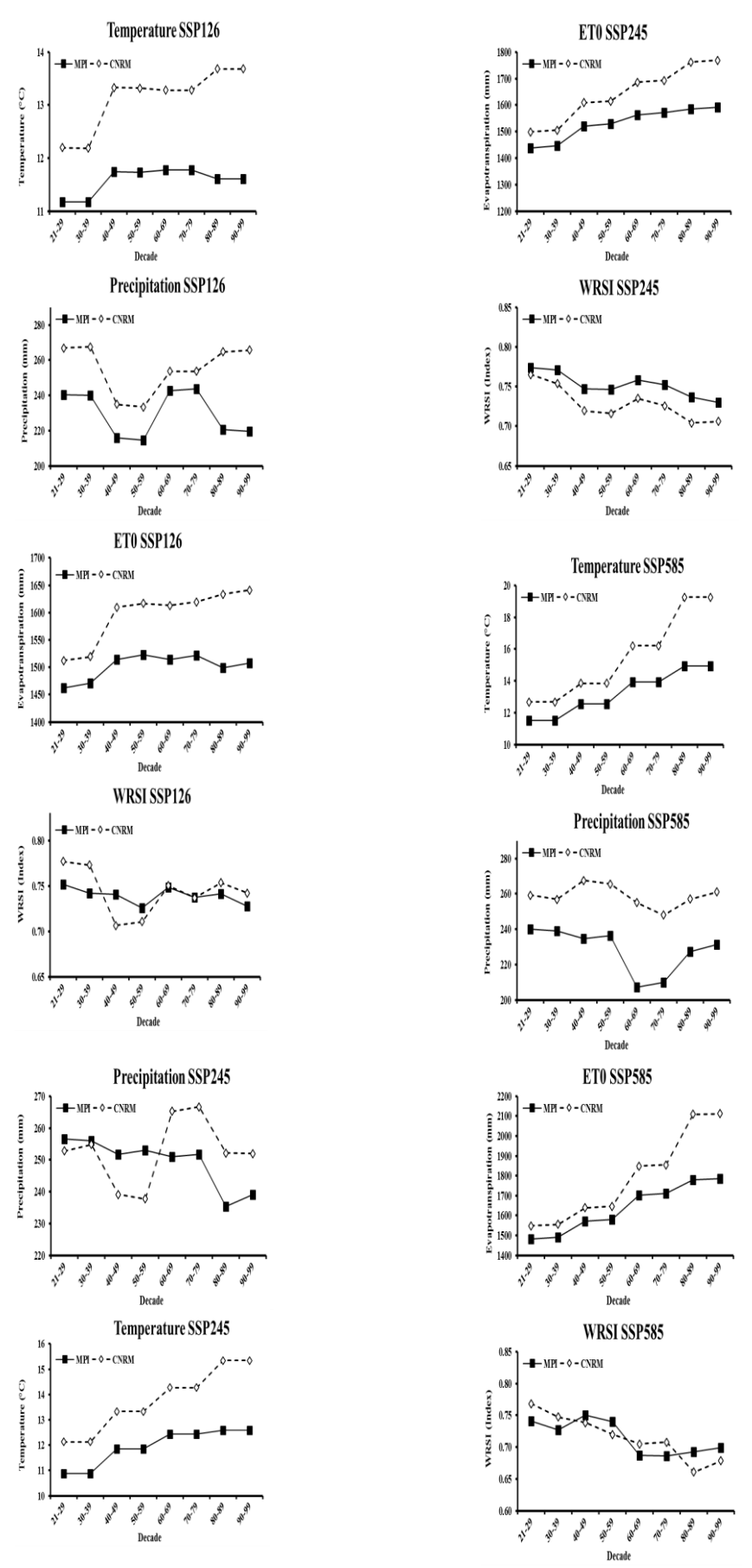
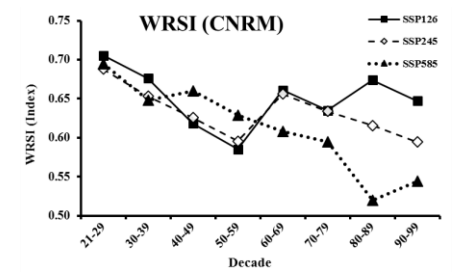


Fig. 2. Ten-year changes in evapotranspiration, temperature, precipitation, and water demand satisfaction index.



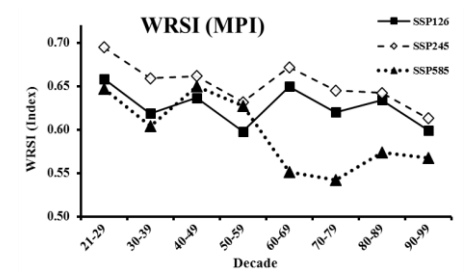
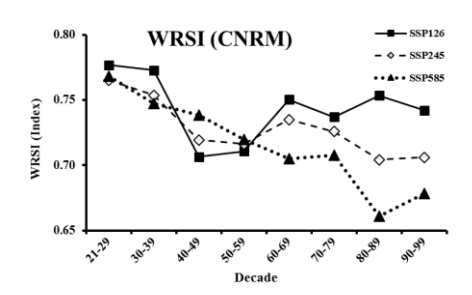


Fig. 3. Trend of changes in the water demand satisfaction index before supplementary irrigation.



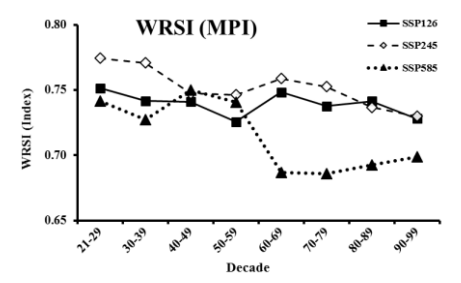
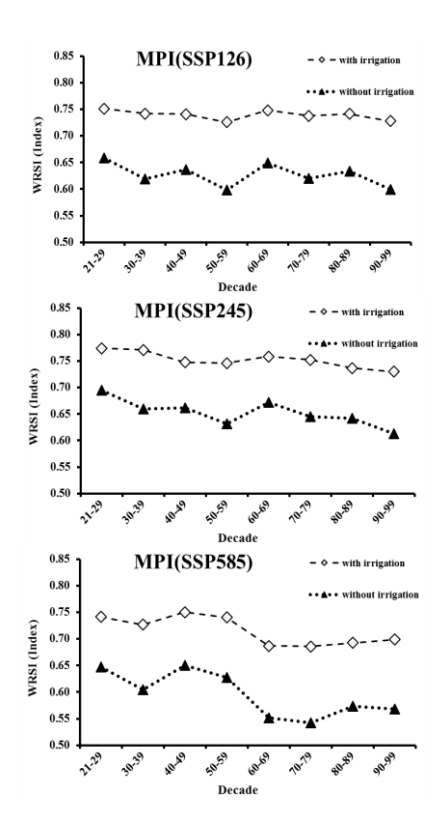


Fig. 4. Trend of changes in the water demand satisfaction index after supplementary irrigation.



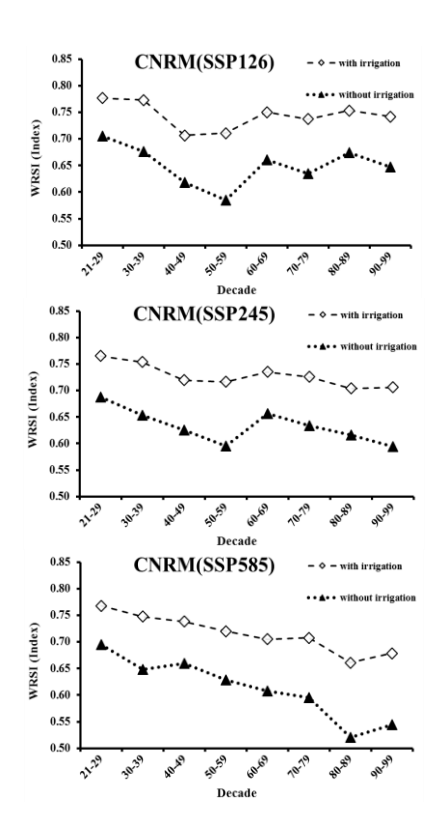


Fig. 5. 10-year changes in WRSI before and after supplementary irrigation.

The comparison between the two tables indicates a clear difference in irrigation needs as dictated by the different climate models. In both tables, the CNRM-CM6-1 and MPI-ESM1-2LR models predict varying WRSI values over the decadal years, reflecting each model's distinct climate

forecasts. The variations in supplementary irrigation values indicate efficiency in water management strategies tailored to each model's predictions, reflecting on the capability to maintain acceptable WRSI levels.

Table 2. the supplementary irrigation schedule based on WRSI values with the CNRM-CM6-1 model and considering the SSP2-4.5 scenario.

Deca	Autumn	Supplementa	WRS	Improv	Deca	Autumn	Supplementa	WRS	Improv
2021 -	-	60	0.78	0.82	2061	-	50	0.78	0.81
2022 -	-	60	0.72	0.77	2062	-	60	0.69	0.73
2023 -	-	50	0.81	0.84	2063	-	50	0.78	0.80
2024 -	-	50	0.76	0.77	2064	-	40	0.71	0.72
2025 -	20	50	0.32	0.60	2065	15	45	0.31	0.57
2026 -	-	60	0.79	0.83	2066	-	50	0.79	0.82
2027 -	-	50	0.80	0.83	2067	-	40	0.81	0.83
2028 -	-	70	0.71	0.79	2068	-	70	0.71	0.78
2029 -	-	80	0.51	0.64	2069 -	-	80	0.47	0.59
2030 -	-	50	0.83	0.85	2070 -	-	40	0.82	0.84
2031 -	15	55	0.50	0.70	2071 -	20	50	0.48	0.69
2032 -	-	50	0.83	0.86	2072 -	-	40	0.85	0.87
2033 -	-	50	0.81	0.84	2073 -	-	40	0.82	0.83
2034 -	-	60	0.59	0.63	2074 -	-	50	0.56	0.61
2035 -	15	55	0.37	0.67	2075 -	20	50	0.36	0.60
2036 -	-	50	0.83	0.86	2076 -	-	50	0.85	0.87
2037 -	-	60	0.66	0.71	2077 -	-	60	0.58	0.63
2038 -	-	70	0.66	0.72	2078 -	-	60	0.59	0.64
2039 -	25	55	0.46	0.70	2079 -	20	50	0.44	0.68
2040	20	50	0.59	0.73	2080 -	10	40	0.53	0.69
2041	-	60	0.75	0.79	2081 -	-	40	0.76	0.78
2042	-	60	0.61	0.68	2082 -	-	60	0.59	0.65
2043	-	60	0.75	0.79	2083 -	-	50	0.75	0.79
2044	-	50	0.64	0.67	2084 -	-	40	0.61	0.64
2045	20	50	0.30	0.59	2085 -	15	45	0.29	0.59
2046	-	60	0.75	0.80	2086 -	-	50	0.75	0.78
2047	-	50	0.78	0.81	2087 -	-	40	0.78	0.81
2048	-	70	0.66	0.75	2088 -	-	60	0.65	0.73
2049	-	80	0.44	0.59	2089 -	-	70	0.44	0.58
2050	-	50	0.75	0.78	2090 -	-	40	0.76	0.77
2051	15	55	0.44	0.68	2091 -	15	45	0.42	0.66
2052	-	60	0.81	0.85	2092 -	-	40	0.85	0.87
2053	-	50	0.78	0.81	2093 -	-	40	0.79	0.81
2054	-	60	0.53	0.59	2094 -	-	50	0.53	0.59
2055	15	65	0.35	0.59	2095 -	20	50	0.34	0.56
2056	-	60	0.82	0.85	2096 -	-	50	0.82	0.85
2057	-	70	0.53	0.60	2097 -	-	50	0.53	0.59
2058	15	55	0.54	0.73	2098 -	15	45	0.54	0.70
2059	20	60	0.40	0.67	2099 -	20	50	0.38	0.66
2060	15	55	0.52	0.69					

Table 3. the supplementary irrigation schedule based on WRSI values with the MPI-ESM1-2LR model and considering the SSP2-4.5 scenario.

Decade (year)	Autumn Irrigation (mm)	Supplementary irrigation(mm)	WRSI	Improved WRSI	Decade (year)	Autumn Irrigation (mm)	Supplementary irrigation(mm)	WRSI	Improved WRSI
2021 - 2022	-	60	0.78	0.82	2061 - 2062	-	60	0.78	0.81
2022 - 2023	-	70	0.73	0.79	2062 - 2063	-	70	0.71	0.77
2023 - 2024	-	60	0.81	0.84	2063 - 2064	-	60	0.81	0.84
2024 - 2025	-	60	0.77	0.80	2064 - 2065	-	50	0.76	0.79
2025 - 2026	15	65	0.34	0.58	2065 - 2066	20	50	0.31	0.61
2026 - 2027	-	70	0.77	0.83	2066 - 2067	-	60	0.78	0.83
2027 - 2028	-	60	0.80	0.84	2067 - 2068	-	60	0.79	0.83
2028 - 2029	-	80	0.71	0.80	2068 - 2069	-	70	0.71	0.79
2029 - 2030	-	80	0.54	0.66	2069 - 2070	-	80	0.50	0.63
2030 - 2031	-	60	0.81	0.85	2070 - 2071	-	50	0.83	0.85
2031 - 2032	20	60	0.51	0.73	2071 - 2072	25	55	0.49	0.71
2032 - 2033	-	60	0.81	0.85	2072 - 2073	-	60	0.84	0.87
2033 - 2034	-	60	0.80	0.84	2073 - 2074	-	60	0.79	0.83
2034 - 2035	-	70	0.61	0.68	2074 - 2075	-	70	0.58	0.64
2035 - 2036	20	60	0.37	0.70	2075 - 2076	-	80	0.36	0.65
2036 - 2037	-	60	0.81	0.85	2076 - 2077	-	60	0.82	0.86
2037 - 2038	-	70	0.70	0.76	2077 - 2078	-	70	0.64	0.71
2038 - 2039	15	55	0.69	0.74	2078 - 2079	-	70	0.64	0.71
2039 - 2040	-	80	0.48	0.71	2079 - 2080	20	60	0.46	0.70
2040 – 2041	-	70	0.59	0.65	2080 - 2081	20	50	0.56	0.69
2041 – 2042	-	60	0.77	0.81	2081 - 2082	-	60	0.74	0.79
2042 – 2043	-	70	0.69	0.76	2082 - 2083	-	70	0.65	0.73
2043 – 2044	-	60	0.80	0.84	2083 - 2084	-	60	0.78	0.82
2044 – 2045	-	60	0.74	0.77	2084 - 2085	-	50	0.71	0.73
2045 – 2046	20	60	0.31	0.59	2085 - 2086	15	55	0.30	0.60
2046 – 2047	-	70	0.76	0.82	2086 - 2087	-	70	0.75	0.81
2047 2047 – 2048	-	60	0.78	0.82	2087 - 2088	-	60	0.77	0.81
2048 2048 – 2049	-	80	0.70	0.79	2088 - 2089	-	80	0.70	0.79
2049 2049 – 2050	-	80	0.49	0.63	2089 - 2090	-	80	0.46	0.60
2050 –	-	60	0.80	0.84	2090 -	-	60	0.80	0.83
2051 2051 –	20	60	0.48	0.71	2091 2091 - 2092	20	60	0.47	0.70
2052 2052 –	-	60	0.81	0.85	2092 -	-	60	0.82	0.86
2053 2053 –	-	60	0.78	0.82	2093 2093 -	-	60	0.78	0.82
2054 2054 –	-	70	0.57	0.63	2094 2094 -	-	70	0.53	0.61
2055 2055 –	20	60	0.35	0.65	2095 2095 -	15	65	0.35	0.65
2056 2056 –	-	60	0.81	0.85	2096 2096 -	-	60	0.81	0.85
2057 2057 –	-	70	0.68	0.74	2097 2097 -	-	70	0.58	0.66
2058 2058 –	_	70	0.60	0.67	2098 2098 -	_	70	0.57	0.65
2059 2059 –	20	60	0.44	0.69	2099 2099 -	20	60	0.42	0.68
2060 2060 –	15	55		0.69	2100	20	50	U <b>r</b> ∠	0.00
2061	13	JJ	0.56	0.09					

For rain-fed wheat around Tabriz, baseline productivity falls within 900-1200 kg/ha. That is average productivity under today's climatic conditions with favorable precipitation and thermal regime in the grow season supportive of wheat development. Yet, where global change is amplified, future decreases in the WRSI suggest severe threats are being presented to future development of wheat within the area. Averaged across under the medium and high emission paths of greenhouse gases under the scenarios of RCP 4.5 and RCP 8.5, respectively, wheat yield decreases of 15-30% are projected through the year 2100. Decreases in WRSI under warmer temperature and reduced precipitation enhance water stress during the critical development phase of wheat, more notably during flowering and grain development. This decline in yield shows the susceptibility of rainfed wheat systems to climate change and the imperative for adaptation measures. The findings in this research highlights the need for proper water management, particularly in areas such as Tabriz, where water is already in short supply and highly unreliable. Supplemental irrigation during key growth periods, for instance, at the grain-filling stage, would be critical in sustaining or enhancing yield potential. Research has proved that supplementary irrigation in small quantities even during years of drought can successfully mitigate water stress, enhance crop performance and stability, and enhance yield.

Moreover, the findings of the current study showed that the WRSI is directly affected by climate change, particularly the reduction in rainfall and the increase in evapotranspiration and temperature in the future. Analysis of the 80-year time series of 2021-2100 illustrated that in all examined climate scenarios including SSP1-2.6, SSP2-4.5, and SSP5-8.5, the WRSI value has decreased in the final decades. This decrease was more severe in the SSP5-8.5 scenario, which represents the highest level of greenhouse gas emissions, and in some cases reached below 50%, which, according to the FAO classification, indicates moderate to severe water stress conditions for the crop (Sultan et al., 2010). Tarnavsky et al. (2018) also reported similar results, showing that with the decrease in rainfall and the increase in temperature, the WRSI value decreased, and the performance of rainfed crops was under stress. So, supplementary irrigation during critical growth stages such as flowering and grain filling was also suggested as an effective solution to reduce water stress, which is fully consistent with the results of the present research. Accordingly, in the current research, the application

of supplementary irrigation, especially during the critical growth stages of rainfed wheat led to a

significant improvement in WRSI in all decades. In many years, the WRSI index increased by 10 to 30 percent due to one or two irrigation events, and in some specific cases, even an increase above 90% was recorded. These findings indicate that ensuring moisture availability during the critical growth periods of the plant can play a decisive role in the sustainability of crop yields. Additionally, Farre and Faci (2006) and Pala et al. (2007) stated that a supplementary irrigation at the grain filling stage in rainfed conditions can increase wheat yield by up to 30%, and this effect is even greater in drier years. In the present study, the percentage improvement in the WRSI index after irrigation in some dry decades also reached over 30%, indicating the importance of the targeted irrigation strategy in critical growth periods of rainfed plants. Also, comparative analysis between climate models showed that the WRSI index in the MPI-ESM1-2-LR model had a more uniform but decreasing trend in severe scenarios, while the CNRM-CM6-1 model simulated higher WRSI values in the SSP2-4.5 scenario, which is consistent with the results of Zareian et al. (2024) and Hosseini-Moghari et al. (2021) regarding the higher accuracy of the CNRM model in semi-arid climates of Iran. Overall, the results of this study emphasize that in the coming decades, without management interventions such as supplementary irrigation, the rainfed agricultural sector in dry and semi-arid regions, especially in northwestern Iran, will face serious challenges. The use of targeted supplementary irrigation based on WRSI analysis can be used as an effective strategy to reduce climate risk and maintain sustainable performance of rainfed crops.

### Conclusion

The obtained results of the current research highlight the crucial role of supplementary irrigation in sustaining rainfed agriculture, particularly in regions like Tabriz, where climate change impacts are noticeable. This study analyzes climate scenarios from 2021 to 2100, utilizing Representative Concentration Pathways scenarios including SSP2-4.5 and SSP5-8.5. Also, LSTM and its advanced variant, the FLF-LSTM, provided robust tools to predict the WRSI with improved accuracy. This model integration enabled a comprehensive understanding of water demand shifts under varying climate scenarios. The obtained results emphasizes the greater importance of supplementary irrigation during the grain filling stage for rainfed wheat. At this stage, the plants demand maximum water to develop high-yielding research identifies The supplementary irrigation values necessary to counteract water deficits anticipated for these crucial growth phases. Furthermore, the results reveal that the future impacts of climate change, especially under the pessimistic SSP5-8.5 scenario, could severely threaten rainfed agriculture in Tabriz. Reduced rainfall and increased temperatures will likely lead to decreased WRSI and crop yields. Yet, by employing supplementary irrigation strategies, these negative effects can be mitigated. Improved WRSI metrics, achieved through targeted water applications, demonstrate the potential to stabilize and even enhance yields under drought conditions. Conclusively, the research highlights the imperative of adopting supplementary irrigation as an integral component of future agricultural strategies in climate-sensitive regions.

# Consent for publication:

All authors declare their consent for publication.

#### **Author contribution:**

The manuscript was edited and revised by all authors.

#### **Conflicts of Interest:**

The author declares no conflict of interest.

#### References

- Abo-Yousef, M., Abd Elaty, M., Sorour, F., Salem, M., Talha, I., & Bahgt, M. (2024). Environmental Stability and Adaptation of Several Rice (Oryza Sativa L.) Cultivars with Different Climate Change. Egyptian Journal of Agronomy, 46(1), 103-113.
- Allen, R. G., Pereira, L. S., Raes, D., & Smith, M. (1998). Crop evapotranspiration: Guidelines for computing crop water requirements (FAO Irrigation and Drainage Paper No. 56). Rome: Food and Agriculture Organization of the United Nations.
- Bauer, A., Black, A. L., & Smika, D. E. (1984). Agricultural climatic data for the United States Great Plains. USDA Agricultural Research Service Bulletin No. 10.
- Chen, H., Zhang, Y., Liu, S., & Zhao, M. (2023). Improving evapotranspiration prediction in arid regions using hybrid loss functions and deep LSTM models. Journal of Hydrology, 619, 129334.
- Chen, X., Xiao, D., Qi, Y., Shi, Z., Bai, H., Lu, Y., Zhang, M., Pan, P., Ren, D., Yin, X., Li, R. (2025). Projected future changes in extreme climate indices affecting rice production in China using a multimodel ensemble of CMIP6 projections. Frontiers in Plant Science. 17;16:1595367.
- Doorenbos, J., & Kassam, A. H. (1979). *Yield Response to Water*. FAO Irrigation and Drainage Paper No. 33. Rome: Food and Agriculture Organization of the United Nations.
- English, M., & Raja, S. N. (1996). Perspectives on deficit irrigation. Agricultural Water Management, 32(1), 1– 14.

- Erekul, O, Gotz, KP and Gurbuz, T. 2012. Effect of supplemental irrigation on yield and breadmaking quality of wheat (Triticum aestivum L.) varieties under the Mediterranean climatical conditions. Turkish Journal of Field Crops, 17(1): 78-86.
- Farre, I., & Faci, J. M. (2006). Comparative response of winter and spring barley to deficit irrigation in a Mediterranean environment. Agricultural Water Management, 84(3), 261–271.
- Fereres, E and Soriano, MA. (2007). *Deficit irrigation for reducing agricultural water use*. Special issue on integrated approaches to sustain and improve plant production under drought stress. Journal of Experimental Botany, 58: 147–159.
- Fouad, H. (2018). Correlation, Path and Regression Analysis in Some Bread Wheat (Triticum aestivum L) Genotypes under Normal Irrigation and Drought Conditions. Egyptian Journal of Agronomy, 40(2), 133-144.
- Frere, M and Popov, G. (1986). Early agrometeorological crop yield assessment. FAO Plant Production and Protection Paper 73. Food and Agriculture Organization of the United Nations, Rome, Italy.
- Giorgetta, M.A., Jungclaus, J.H., Reick, C.H., Legutke, S., Bader, J., Böttinger, M., Brovkin, V., Crueger, T., Esch, M., Fieg, K. (2013). The MPI-ESM1-2-LR Model and Its Application in Climate Projections. Journal of Climate, 26(18): 6756-6772.
- Hosseini-Moghari, S.M., Ahmadi, A., Tavakol-Davani, H., & Ghaffari, G. (2021). Assessment of climate change impacts over Iran using CMIP6 models. Climate Risk Management, 33, 100329.
- Khosravi, H., Yazdanpanah, M., & Forouzani, M. (2020). *Climate change discourse among Iranian farmers*. Climatic Change, 162(3), 1235–1250.
- Kouadio, L., Zhang, Y., Wang, Y., & Li, X. (2023). Evaluation of CMIP6 precipitation simulations across different climatic zones: Uncertainty and model intercomparison. Atmosphere, 14(11), 1478.
- Lobell, D. B., Schlenker, W., & Costa-Roberts, J. (2011). *Climate Trends and Global Crop Production Since* 1980. Science, 333(6042), 616–620.
- McMaster, G. S., & Wilhelm, W. W. (1997). *Growing degree-days: one equation, two interpretations*. Agricultural and Forest Meteorology, 87(4), 291–300. https://doi.org/10.1016/S0168-1923(97)00027-0
- Oweis T., (1997). Supplemental Irrigation: A highly efficient water-use practice. International Center for Agricultural Research in the Dry Areas (ICARDA), Aleppo, Syria.
- Oweis, T, and Hachum, A. (2009). *Optimizing* supplemental irrigation: Tradeoffs between profitability and sustainability. Agricultural Water Management, 96: 511-516.

- Pala, M., Ryan, J., Zhang, H., Singh, M., & Harris, H. (2007). Management options for improving wheat
- Sadek, S.E., and Saba, M.F.A. (2011). *Predicting Impacts of Climate Change on Maize Productivity in Egypt.* Egyptian Journal of Agronomy, 33(1), 83-94.
- Schlenker, W., & Roberts, M. J. (2009). Nonlinear temperature effects indicate severe damages to U.S. crop yields under climate change. Proceedings of the National Academy of Sciences, 106(37), 15594– 15598.
- Semenov, M. A., & Stratonovitch, P. (2010). *Use of multi-model ensembles from global climate models for impact assessments of climate change. Climate Research*, 41(1), 1–14.
- Silva, V, Campos, J, Silva, MT and Azevedo, PV. (2010). Impact of global warming on cowpea bean cultivation in northeastern Brazil. Agricultural Water Management, 97: 1760-1768.
- Soltani, A., Gholipoor, M., Zeinali, E., Soltani, M., & Arabzadeh, M. (2012). Rainfed wheat yield and water use efficiency under different supplemental irrigation scenarios in a semi-arid environment: Field and simulation results. Field Crops Research, 127, 56–67.
- Sultan, B, Bella-Medjo, M, Berg, A, Quirion, P and Janicot, S. (2010). Multi-scales and multi-sites analyses of the role of rainfall in cotton yields in West Africa. International Journal of Climatology, 30: 58–71
- Sultan, B., Roudier, P., Quirion, P., Alhassane, A., Traore, S., Muller, B., Dingkuhn, M., Ciais, P., Guimberteau, M., & Baron, C. (2010). Assessing climate change impacts on sorghum yield in West
- Zareian, M.J., Dehban, H., Gohari, A.& Torabi Haghighi, A. (2024). Assessment of CMIP6 models performance in simulation precipitation and temperature over Iran and surrounding regions. Environmental Monitoring and Assessment. 196, 701.
- Zhang, H., Oweis, T., Pala, M., & Harris, H. (2006). Influence of early supplemental irrigation on root development and grain yield of wheat under dryland conditions. Soil and Tillage Research, 89(1), 1–12.

- yield and water productivity in dry areas. Agricultural Water Management, 93(1-2), 1–10.
- Africa. Environmental Research Letters, 5(1), 014008
- Talebi, H., Samadianfard, S. (2024). Integration of machine learning and remote sensing for drought index prediction: A framework for water resource crisis management. Earth Science Informatics 17, 4949–4968.
- Tarnavsky, E., Chavez, E and Boogaard, H. (2018). Agro-meteorological risks to maize production in Tanzania: Sensitivity of an adapted Water Requirements Satisfaction Index (WRSI) model to rainfall. International Journal of Applied Earth Observation and Geoinformation, 73: 77–87.
- Tavakoli, A.R. and Oweis, T.Y. (2004). The role of supplemental irrigation and nitrogen in producing bread wheat in the highlands of Iran. Agricultural Water Management. 65: 225-236.
- Verdin, J and Klaver, R. (2002). *Grid-cell-based crop* water accounting for the famine early warning system. Hydrological Processes, 16: 1617-1630.
- Voldoire, A., Saint-Martin, D., Sénési, S., Decharme, B., Alias, A., Chevallier, M., Colin, J., Guérémy, J.F., Michou, M., Moine, M.P. (2019). The CNRM-CM6-1 Earth System Model: Description and Evaluation. Climate Dynamics, 52, 1497–1536.
- Wang, Y., Zhang, Q., Liu, F., & Li, X. (2021). A novel composite loss function for time series forecasting with LSTM networks. Neural Computing and Applications, 33(21), 13761–13776.
- Zhang, X., Ding, Y., Zhu, L., Wan, Y., Chai, M., & Ding, P. (2023). Estimating and forecasting daily reference crop evapotranspiration in China with temperaturedriven deep learning models. Agricultural Water Management, 307, 109268.
- Zhang, Y., Liu, D., Chen, X., Li, M., & Wang, J. (2022). Improving time-series prediction of evapotranspiration using FLF-LSTM: A fused loss function deep learning approach. Journal of Hydrology, 610, 127936.